ORIGINAL ARTICLE
DOI: 10.5433/1679-0375.2022v43n1Espp29

Two-step incremental procedure associated with the normal flow technique applied to trusses

Procedimento incremental de dois passos associado à técnica de fluxo normal aplicado a treliças

Luiz Antonio Farani de Souza[1]; Wilson Doná Junior[2];
Everton Luis Consoni da Silva[3]

Abstract

To achieve the nonlinear structural behavior, there is a need to trace of their equilibrium path in the space of load-displacement. Truss systems are commonly implemented in several structural systems, including high-span bridges and bracing of the supporting structure of tall buildings. Our study adapts a two-step method with cubic convergence into an incremental-iterative procedure to analyze the geometric nonlinear behavior of trusses. The solution method is combined with the Linear Arc-Length path-following technique. To find the approximate root of nonlinear equation system in the two-step method, two formulas are used. Structures are discretized using the Positional Finite Element Method and all truss bars are assumed to remain linear elastic. The correction of the nodal coordinates subincrement vector is performed using the Normal Flow technique. A computational algorithm was implemented using the free program Scilab. Our numerical results show that, when compared to the standard and modified Newton-Raphson algorithms, the new algorithm decreases the number of iterations and the computing time in the nonlinear analysis of trusses. Equilibrium paths with force and/or displacement limit points are obtained with good precision.

Keywords: Linear Arc-Length; positional formulation; geometric nonlinearity; Normal Flow technique.

Resumo

Para obter o comportamento não linear de uma estrutura, há a necessidade de traçar sua trajetória de equilíbrio no espaço de carga-deslocamento. Os sistemas treliçados são comumente empregados em vários sistemas estruturais, incluindo pontes com grandes vãos e contraventamento da estrutura po rtante de edifícios altos. Este estudo adapta um método de dois passos com convergência cúbica em um procedimento incremental-iterativo para analisar o comportamento não linear geométrico de treliças. Esse método é combinado com a técnica de continuação Comprimento de Arco Linear. Duas fórmulas são usadas para encontrar a raiz aproximada do sistema de equações não lineares. As estruturas são discretizadas por meio do Método Posicional dos Elementos Finitos e assume-se que todas as barras de treliça permaneçam elásticas lineares. A correção do vetor de subincremento de coordenadas nodais é realizada pela técnica de Fluxo Normal. Um algoritmo computacional foi implementado utilizando o programa livre Scilab. Os resultados numéricos mostram que, quando comparado com os algoritmos de Newton-Raphson Padrão e Modificado, o novo algoritmo diminui o número de iterações e o tempo de processamento nas análises não lineares de treliças. As trajetórias de equilíbrio com pontos limites de força e/ou de deslocamento são obtidas com boa precisão.

Palavras-chave: Comprimento de Arco Linear; formulação posicional; não linearidade geométrica; técnica de Fluxo Normal.

[1] Prof. Dr., Civil Engineering Course, UTFPR, Apucarana, PR, Brazil, E-mail: lasouza@utfpr.edu.br
[2] Master's Student, Graduate Program in Civil Engineering, UEM, Maringá, PR, Brazil, E-mail: wilsondonajunior@gmail.com
[3] Master's Student, Graduate Program in Civil Engineering, UEM, Maringá, PR, Brazil, E-mail: everton01.1995@gmail.com

Introduction

Finding effective solutions for problems involving large deformations of dead loads have been considered a serious and difficult challenge from the numerical and analytical perspectives. Several studies have sought for schemes capable of achieving the nonlinear equilibrium path in the load-displacement space (KOOHESTANI, 2013; LEON *et al*., 2011; TURCO *et al*., 2020), which requires enough efficiency to cross the critical and buckling points (REZAIEE-PAJAND; NASERIAN, 2015). Figure 1 shows the nonlinear response of a structural system in which a given displacement component may either increase or decrease along the path, including load limit points 1 and 4, displacement limit points 2 and 3 and the failure point 5. Load limit points occur when a local maximum or minimum load is reached on the load-displacement curve, embedding a horizontal tangent. Displacement limit points occur at vertical tangents on the solution curve (LEON *et al*., 2011).

The mathematical modeling of engineering structures response can provide the nonlinear effects of different sources, including geometric nonlinearities associated to large displacements and strains, as well as nonlinear material responses described by theories such as plasticity, damage, and fracture (MUÑOZ; ROEHL, 2017).

Figure 1 – Critical points in nonlinear equilibrium paths.

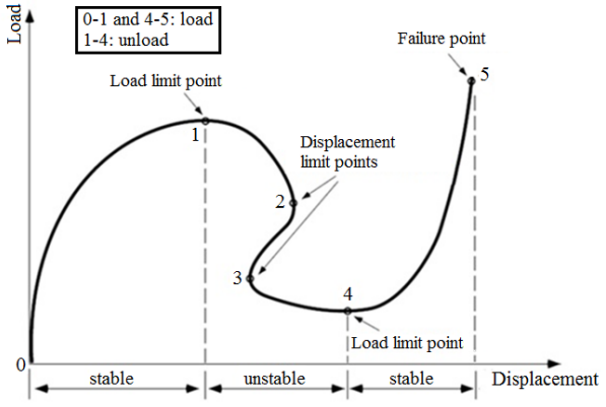

Source: Adapted from Leon *et al*. (2011).

Considering that structures may experience changes in their primary shape before reaching the final strengths, accurately evaluating structures behavior in large displacement cases require a geometrically nonlinear analysis (MOHIT; SHARIFI; TAVAKOLI, 2020). In this scenario, space truss is a structural element widely employed in Structural Engineering (GRECO; FERREIRA, 2009) for the construction of long-range bridge systems, domes, or roofs of structures covering large unobstructed areas, or in the reinforcement of structures (DEHGHANI *et al*., 2020; THAI; KIM, 2009).

The Newton–Raphson method is one of the most powerful and widely used techniques for solving nonlinear problems, so that most iterative algorithms adapted for this end may be regarded as variations of this technique (SAFFARI; MANSOURI, 2011). By means of an incremental-iterative procedure, this method provides the solution of points in the equilibrium path, which may diverge for a limit point due to the ill conditioning of the tangent stiffness matrix, Jacobian matrix, or because the established load level lacks a solution. To solve this problem, the displacement control method was introduced. However, as this strategy provides inaccurate answers for structures with snap-back points, researchers have suggested a more general method for nonlinear structural analysis – the Arc-Length technique (SAFFARI *et al*., 2013).

The literature present numerous approaches for the nonlinear structural analysis of trusses – Saffari and Mansouri (2011) suggested a two-point fourth-order convergence method; Mahdavi *et al*. (2015) proposed an iterative method free from second derivative originated from modified Chebyshev and cubic spline's schemes; Souza *et al*. (2018) proposed new algorithms based on two-step methods with cubic convergence combined with the Linear Arc-Length path-following technique; Mohit, Sharifi and Tavakoli (2020) used six three-step fourth-order convergence iterative schemes; Dehghani *et al*. (2020) proposed an improved perturbation algorithm to refine the classical methods in numerical computing techniques such as the Newton–Raphson method; Souza, Castelani and Shirabayashi (2021a) adapted the Newton-Raphson and Potra-Pták algorithms by combining them with the modified Newton-Raphson method by inserting a condition; and, finally, Souza *et al*. (2021) presented a new algorithm to solve the system of nonlinear equations that describes the static equilibrium of trusses with material and geometric nonlinearities, adapting a three-step method with fourth-order convergence.

Two-step methods, also called predictor–corrector methods (NOOR; AHMAD; JAVEED, 2006), use two formulas to find the approximate function's root. Whereas one formula predicts the root based on the initial estimate (predictor), the second formula gives the correct approximation based on the predicted value (corrector).

Consider a nonlinear equation $f(x) = 0$ with a simple root x^*, where $f : D \subset \mathbb{R} \to \mathbb{R}$ for an open interval D is a

scalar function. Kou, Li and Wang (2006) presented a modified Newton's method for solving nonlinear equations, which has cubic convergence and requires two evaluations of the function $f(x)$ and one evaluation of its first derivative $f'(x)$. The iterative equations for this method are as follows:

$$y^{(k+1)} = x^{(k)} + \frac{f\left(x^{(k)}\right)}{f'\left(x^{(k)}\right)}, \tag{1}$$

$$x^{(k+1)} = y^{(k+1)} - \frac{f\left(y^{(k+1)}\right)}{f'\left(x^{(k)}\right)}, \tag{2}$$

for $k = 0, 1, 2, \ldots$, generating a sequence of iterations which converges to $x^* \in D$. If $f(x)$ has first, second and third derivatives in the interval D, then the method defined by equations (1) and (2) converges cubically to x^* in a neighborhood of x^*. Our study adapts the two-step method proposed by Kou, Li and Wang (2006) into an incremental-iterative procedure to solve the nonlinear equations of the structural problem, thus generating a new algorithm. The solution method is combined with the Linear Arc-Length path-following technique, which adds a constraint equation to the system for calculating the load factor.

Structures were discretized using the Positional Finite Element formulation originally proposed by Coda and Greco (2004). Conventionally, the formulation of the Finite Element Method for solid mechanics comprises the displacement method, in which primary unknowns are nodes displacements. Conversely, the unknowns within the positional formulation are nodes positions. This formulation adopts the Lagrangian description, which describes the kinematics of deformation in terms of a coordinate system, fixed in space.

We developed a computational algorithm, using the free program Scilab, version 6.1.1 (SCILAB, 2021), capable of tracing the load-displacement paths of nonlinear problems with multiple force and displacement points to predict the large deflection behavior of plane and spatial trusses. The truss bars are assumed to have linear elastic behavior.

The nodal coordinate subincrement vector is corrected in the iteration through two strategies: conventional (CRISFIELD, 1991); and Normal Flow (MAXIMIANO; SILVA; SILVEIRA, 2014; RAGON; GÜRDAL; WATSON, 2002). The equilibrium between the internal and external forces in the Normal Flow technique is obtained by performing iterative corrections along of the normal direction to the Davidenko curves (ALLGOWER; GEORG, 1980). This technique is used to accelerate the process of obtaining the approximate solution and/or to overcome the problems of convergence, which can occur at the limit points of the structure equilibrium path.

Studies analyzing nonlinear truss have also applied the positional formulation: Greco and Ferreira (2009) used the logarithmic strain measure to obtain a consistent geometric nonlinear finite element formulation to deal with large strains on space trusses; by comparing the positional formulation of space trusses with the co-rotation formulation, Greco *et al*. (2012) found results with good agreement; Rabelo *et al*. (2018) developed a formulation to describe the viscoelastic mechanical behavior of space trusses; and Felipe *et al*. (2019) proposed the comprehensive ductile-damage model for nonlinear analysis of truss structures.

Structural problem and solution method

The basic problem of nonlinear analysis is to find the equilibrium configuration of a structure that is under the action of an applied load. The system of nonlinear equations that governs the static equilibrium of a structural system with geometrically nonlinear behavior is given by (MAXIMIANO; SILVA; SILVEIRA, 2014):

$$\boldsymbol{g}(\boldsymbol{d}, \lambda) = \boldsymbol{F_{int}}(\boldsymbol{d}) - \lambda \boldsymbol{F_r} = \boldsymbol{0}, \tag{3}$$

where $\boldsymbol{g}$ is the unbalanced force vector, $\boldsymbol{F_{int}}$ is the internal force vector, evaluated as a function of the coordinate vector at the nodal points of structure $\boldsymbol{d}$, $\boldsymbol{F_r}$ is a reference vector characterizing the external load direction and λ is the load parameter. The solution of the system given in equation (3) is obtained by an incremental-iterative scheme. For a sequence of the load parameter λ, a sequence of the respective increment of nodal coordinates $\boldsymbol{d}$ is calculated.

The system has $(n+1)$ unknowns, which are the vector d with n elements and the parameter λ, but only n equations. Thus, the constraint equation $c(\boldsymbol{d}, \lambda) = 0$ is added to the system.

By applying the standard Newton-Raphson method to the system of equations in equation (3) and $c(\boldsymbol{d}, \lambda) = 0$ (LEON *et al*., 2011; SOUZA *et al*., 2018), we obtain the equations (4)-(6) :

$$\frac{\partial \boldsymbol{g}^{(k)}}{\partial \boldsymbol{d}} \delta \boldsymbol{d}^{(k+1)} + \frac{\partial \boldsymbol{g}^{(k)}}{\partial \lambda} \delta \lambda^{(k+1)} = -\boldsymbol{g}^{(k)}, \tag{4}$$

$$\boldsymbol{K}^{(k)} \delta \boldsymbol{d}^{(k+1)} - \delta \lambda^{(k+1)} \boldsymbol{F_r} = -\boldsymbol{g}^{(k)}, \tag{5}$$

$$\left(\frac{\partial c^{(k)}}{\partial \boldsymbol{d}}\right)^T \delta \boldsymbol{d}^{(k+1)} + \frac{\partial c^{(k)}}{\partial \lambda} \delta \lambda^{(k+1)} = -c^{(k)}, \tag{6}$$

with

$$\boldsymbol{d}^{(k+1)} = \boldsymbol{d}^{(k)} + \delta\boldsymbol{d}^{(k+1)}, \tag{7}$$

$$\lambda^{(k+1)} = \lambda^{(k)} + \delta\lambda^{(k+1)}, \tag{8}$$

where $\boldsymbol{K}^{(k)} = \dfrac{\partial \boldsymbol{F_{int}}}{\partial \boldsymbol{d}}$ is the stiffness matrix, which is the Jacobian matrix, and $\delta\lambda^{(k)}$ the load sub-increment. The terms $(k+1)$ and k are used herein to refer to the current and previous iterations, respectively. By isolating the coordinate sub-increment $\delta\boldsymbol{d}^{(k+1)}$ in equation (4) and assuming that $\boldsymbol{K}^{(k)}$ is invertible (LEON *et al*., 2011), we obtain the equation (9):

$$\delta\boldsymbol{d}^{(k+1)} = \delta\boldsymbol{d}_{\boldsymbol{g}}^{(k+1)} + \delta\lambda^{(k+1)}\delta\boldsymbol{d}_{\boldsymbol{r}}^{(k+1)}, \tag{9}$$

where

$$\delta\boldsymbol{d}_{\mathbf{g}}^{(k+1)} = -\left[\boldsymbol{K}\left(\boldsymbol{d}^{(k)}\right)\right]^{-1}\boldsymbol{g}\left(\boldsymbol{d}^{(k)},\,\lambda^{(k)}\right), \tag{10}$$

$$\delta\boldsymbol{d}_{\boldsymbol{r}}^{(k+1)} = \left[\boldsymbol{K}\left(\boldsymbol{d}^{(k)}\right)\right]^{-1}\boldsymbol{F_r}. \tag{11}$$

In equation (10), $\boldsymbol{g}\left(\boldsymbol{d}^{(k)},\lambda^{(k)}\right) = \boldsymbol{F_{int}}\left(\boldsymbol{d}^{(k)}\right) - \lambda^{(k)}\boldsymbol{F_r}$. The usage of equation (9) is referred to herein as the conventional process for the nonlinear solution methodology. In the Normal Flow technique, the equilibrium between the internal and external forces is obtained by performing iterative corrections along of the normal direction to the Davidenko curves (ALLGOWER; GEORG, 1980; RAGON; GÜRDAL; WATSON, 2002; MAXIMIANO; SILVA; SILVEIRA, 2014). With this technique, the expression used to obtain the nodal displacement correction $\delta\boldsymbol{d}^{(k+1)}$ is given by the equation (12):

$$\delta\boldsymbol{d}^{(k+1)} = \delta\boldsymbol{d}_{\boldsymbol{g}}^{(k+1)} + \delta\lambda^{(k+1)}\delta\boldsymbol{d}_{\boldsymbol{r}}^{(k+1)} - \frac{\left(\delta\boldsymbol{d}_{\boldsymbol{g}}^{(k+1)} + \delta\lambda^{(k+1)}\delta\boldsymbol{d}_{\boldsymbol{r}}^{(k+1)}\right)^{T}\delta\boldsymbol{d}_{\boldsymbol{r}}^{(k+1)}}{\delta\boldsymbol{d}_{\boldsymbol{r}}^{(k+1)^{T}}\delta\boldsymbol{d}_{\boldsymbol{r}}^{(k+1)}}\delta\boldsymbol{d}_{\boldsymbol{r}}^{(k+1)}. \tag{12}$$

The increments of nodal coordinates ($\boldsymbol{\Delta d}$) and load ($\Delta\lambda$) are determined by the equations (13) and (14), respectively:

$$\boldsymbol{\Delta d}^{(k+1)} = \boldsymbol{\Delta d}^{(k)} + \boldsymbol{\delta d}^{(k+1)}, \tag{13}$$

$$\Delta\lambda^{(k+1)} = \Delta\lambda^{(k)} + \delta\lambda^{(k+1)}, \tag{14}$$

By combining the solution with the Linear Arc-Length path-following technique, we obtained the constraint equation c in iteration $(k+1)$, given by:

$$c^{(k+1)} = \delta\boldsymbol{d}^{(k+1)^{T}}\Delta\boldsymbol{d}^{(0)} = 0. \tag{15}$$

With the substitution of the sub-increment $\delta\boldsymbol{d}^{(k+1)}$ of equation (9) in equation (15), we obtain the expression for the load sub-increment $\delta\lambda^{(k+1)}$, given in equation (16), for $k > -1$:

$$\delta\lambda^{(k+1)} = -\frac{\delta\boldsymbol{d}_{\boldsymbol{g}}^{(k+1)^{T}}\Delta\,\boldsymbol{d}^{(0)}}{\delta\boldsymbol{d}_{\boldsymbol{r}}^{(k+1)^{T}}\Delta\,\boldsymbol{d}^{(0)}}. \tag{16}$$

Kou, Li and Wang (2006) modified the Newton-Raphson method and developed a two-step method with cubic convergence, which consists of two evaluations of the function and requires only the calculation of first order derivatives. To solve the structural problem given by equation (3) and $c(\boldsymbol{d},\lambda) = 0$, we adapted this method, obtaining the following new incremental-iterative scheme with Normal Flow technique, equations (17)-(21):

$$\boldsymbol{y}^{(k+1)} = \boldsymbol{d}^{(k)} + \delta\boldsymbol{d}_1^{(k+1)} \tag{17}$$

$$\delta\boldsymbol{d}_1^{(k+1)} = \delta\lambda_1^{(k+1)}\delta\boldsymbol{d}_{\boldsymbol{r}}^{(k+1)} + \delta\boldsymbol{d}_{\boldsymbol{g}}^{(k+1)} - \frac{\left(\delta\boldsymbol{d}_{\boldsymbol{g}}^{(k+1)} + \delta\lambda_1^{(k+1)}\delta\boldsymbol{d}_{\boldsymbol{r}}^{(k+1)}\right)^{T}\delta\boldsymbol{d}_{\boldsymbol{r}}^{(k+1)}}{\delta\boldsymbol{d}_{\boldsymbol{r}}^{(k+1)^{T}}\delta\boldsymbol{d}_{\boldsymbol{r}}^{(k+1)}}\delta\boldsymbol{d}_{\boldsymbol{r}}^{(k+1)} \tag{18}$$

$$\delta\boldsymbol{d}_2^{(k+1)} = \delta\lambda_2^{(k+1)}\delta\boldsymbol{d}_{\boldsymbol{r}}^{(k+1)} + \delta\boldsymbol{d}_{\boldsymbol{gy}}^{(k+1)} - \frac{\left(\delta\boldsymbol{d}_{\boldsymbol{gy}}^{(k+1)} + \delta\lambda_2^{(k+1)}\delta\boldsymbol{d}_{\boldsymbol{r}}^{(k+1)}\right)^{T}\delta\boldsymbol{d}_{\boldsymbol{r}}^{(k+1)}}{\delta\boldsymbol{d}_{\boldsymbol{r}}^{(k+1)^{T}}\delta\boldsymbol{d}_{\boldsymbol{r}}^{(k+1)}}\delta\boldsymbol{d}_{\boldsymbol{r}}^{(k+1)} \tag{19}$$

$$\boldsymbol{d}^{(k+1)} = \boldsymbol{d}^{(k)} + \delta\boldsymbol{d}_1^{(k+1)} - \delta\boldsymbol{d}_2^{(k+1)}, \tag{20}$$

$$\lambda^{(k+1)} = \lambda^{(k)} + \delta\lambda_2^{(k+1)}, \tag{21}$$

where $\delta\boldsymbol{d}_{\boldsymbol{gy}}^{(k+1)} = -\left[\boldsymbol{K}\left(\boldsymbol{d}^{(k)}\right)\right]^{-1}\boldsymbol{g}\left(\boldsymbol{y}^{(k+1)},\lambda^{(k)}\right)$. Given that the iteration cycle requires a single factoring at its beginning, the explicit calculation of $\left[\boldsymbol{K}\left(\boldsymbol{d}^{(k)}\right)\right]^{-1}$ is avoided by solving the systems of linear equations via LU factorization. The equation for the initial load increment, predicted solution, is given by equation (22), for $k = -1\%$:

$$\Delta\lambda^{(0)} = \frac{\Delta l}{||\delta\boldsymbol{u_r}||}, \tag{22}$$

where Δl represents the Arc-Length increment, which can be used as a control parameter in the current load step (CRISFIELD, 1991), according to the expression by equation (23) :

$$\Delta l = {}^{0}\Delta\, l \left(\frac{Nd}{{}^{t}k} \right)^{0.5}, \tag{23}$$

where ${}^{0}\Delta\, l$ is the arc length increment in the initial load step, Nd is the number of iterations desired for the convergence of the current iterative process and ${}^{t}k$ is the number of iterations required for converging the previous load step. Typical values for Nd may vary between 3 and 10 (CRISFIELD, 1991).

The end of the iterative process, correction of the predicted solution, indicates a new equilibrium position for the structural system. Two convergence criteria are considered. The first criterion is calculated as a function of the unbalanced load vector g and the reference load vector $\boldsymbol{F_r}$:

$$||\boldsymbol{g}|| \leq tol_1.||\boldsymbol{F}_r||. \tag{24}$$

The second criterion is written as a function of the sub-increment vector of nodal coordinates $\delta\boldsymbol{d}$ and the increment vector of nodal coordinates $\boldsymbol{\Delta d}$:

$$||\delta\boldsymbol{d}|| \leq tol_2.||\Delta\boldsymbol{d}||. \tag{25}$$

In equations (24) and (25), $||.||$ is the Euclidean norm and tol_1 and tol_2 are the tolerances provided by the user. The nodal displacement vector $\boldsymbol{u}^{(k+1)}$ is calculated by equation (26):

$$\boldsymbol{u}^{(k+1)} = \boldsymbol{d}^{(k+1)} - {}^{0}\boldsymbol{d}, \tag{26}$$

where $\boldsymbol{d}^{(k+1)}$ is the nodal coordinate vector converged in the current load step and ${}^{0}\boldsymbol{d}$ is the nodal coordinate vector at the initial position, corresponding to the undeformed configuration of the structure.

The proposed algorithm of the solution method is shown in Algorithm, adapted from the method developed by Kou, Li and Wang (2006) associated with the Linear Arc-Length path-following technique and the Normal Flow strategy. Input parameters considered were: initial arc length (${}^{0}\Delta l$); maximum number of iterations in each step load (k_{max}); required number of iterations (Nd); tolerances (tol_1 and tol_2); load increment (ΔP); maximum number of load steps (LS_{max}); and the nodal coordinate vector at the initial position (${}^{0}\boldsymbol{d}$). In turn, output parameters were: nodal coordinate vector ($\boldsymbol{d}$); total load parameter (λ); total number of load steps (LS); total number of iterations (k_{total}); nodal displacement vector ($\boldsymbol{u}$); average number of iterations (k_{av}); and processing time in seconds (t).

To consider the conventional process for calculating the sub-increment vector of nodal coordinates according to equation (9), line 23 is replaced by $\boldsymbol{\delta d}_1 \leftarrow \delta\lambda_1\boldsymbol{\delta d_r} + \boldsymbol{\delta d_g}$ and line 28, by $\boldsymbol{\delta d}_2 \leftarrow \delta\lambda_2\boldsymbol{\delta d_r} + \boldsymbol{\delta d_{gy}}$ in the proposed algorithm in Algorithm 1.

Algorithm 1: Solution method

Input: LS_{max}, k_{max}, ΔP, ${}^{0}\Delta l$, tol_1, tol_2, Nd, ${}^{0}\boldsymbol{d}$
Output: $\boldsymbol{d}$, $\boldsymbol{u}$, LS, λ, k_{total}, k_{av}, t

1 **begin**
2 $\quad \boldsymbol{d} \leftarrow {}^{0}\boldsymbol{d}$ $\boldsymbol{\Delta d} \leftarrow \boldsymbol{0}$, $\lambda \leftarrow 0$, $k_{total} \leftarrow 0$, $\Delta l \leftarrow {}^{0}\Delta l$
3 $\quad \text{aux}_1 \leftarrow tol_1||\boldsymbol{F_r}||$
4 $\quad$ tic() (starts a timer)
5 $\quad$ **for** $LS \leftarrow 1, \ldots, LS_{max}$ **do**
6 $\quad\quad$ Decomposition of $\boldsymbol{K}$ in matrices $\boldsymbol{L}$ and $\boldsymbol{U}$ (LU factorization)
7 $\quad\quad \textbf{aux}_2 \leftarrow [\boldsymbol{L}]^{-1}\boldsymbol{F_r}$
8 $\quad\quad \boldsymbol{\delta d_r} \leftarrow [\boldsymbol{U}]^{-1}\textbf{aux}_2$
9 $\quad\quad \Delta\lambda^{(0)} \leftarrow \dfrac{\Delta 1}{||\boldsymbol{\delta d_r}||}$
10 $\quad\quad$ **if** $\boldsymbol{\Delta d}^T\boldsymbol{\delta d_r} < 0$ **then**
11 $\quad\quad\quad \Delta\lambda^{(0)} \leftarrow -\Delta\lambda^{(0)}$
12 $\quad\quad$ **end**
13 $\quad\quad \boldsymbol{\Delta d}^{(0)} \leftarrow \Delta\lambda^{(0)}\boldsymbol{\delta d_r}$
14 $\quad\quad \boldsymbol{\Delta d} \leftarrow \boldsymbol{\Delta d}^{(0)}$
15 $\quad\quad \boldsymbol{g} \leftarrow (\lambda + \Delta\lambda)\boldsymbol{F_r} - \boldsymbol{F_{int}}(\boldsymbol{d} + \boldsymbol{\Delta d})$
16 $\quad\quad$ **for** $k \leftarrow 1, \ldots, k_{max}$ **do**
17 $\quad\quad\quad$ Decomposition of $\boldsymbol{K}$ in matrices $\boldsymbol{L}$ and $\boldsymbol{U}$ (LU factorization)
18 $\quad\quad\quad \textbf{aux}_2 \leftarrow [\boldsymbol{L}]^{-1}\boldsymbol{F_r}$
19 $\quad\quad\quad \boldsymbol{\delta d_r} \leftarrow [\boldsymbol{U}]^{-1}\,\textbf{aux}_2$
20 $\quad\quad\quad \textbf{aux}_2 \leftarrow [\boldsymbol{L}]^{-1}\boldsymbol{g}$
21 $\quad\quad\quad \boldsymbol{\delta d_g} \leftarrow [\boldsymbol{U}]^{-1}\,\textbf{aux}_2$
22 $\quad\quad\quad \delta\lambda_1 \leftarrow -\dfrac{(\boldsymbol{\Delta d}^{(0)T}\boldsymbol{\delta d_g})}{(\boldsymbol{\Delta d}^{(0)T}\boldsymbol{\delta d_r})}$
23 $\quad\quad\quad \boldsymbol{\delta d}_1 \leftarrow \delta\lambda_1\boldsymbol{\delta d_r} + \boldsymbol{\delta d_g} - \dfrac{(\boldsymbol{\delta d_g} + \delta\lambda_1\boldsymbol{\delta d_r})^T\boldsymbol{\delta d_r}}{\boldsymbol{\delta d_r}^T\boldsymbol{\delta d_r}}\boldsymbol{\delta d_r}$
24 $\quad\quad\quad \boldsymbol{g} \leftarrow (\lambda + \Delta\lambda + \delta\lambda_1)\boldsymbol{F_r} - \boldsymbol{F_{int}}(\boldsymbol{d} + \boldsymbol{\Delta d} - \boldsymbol{\delta d}_1)$
25 $\quad\quad\quad \textbf{aux}_2 \leftarrow [\boldsymbol{L}]^{-1}\boldsymbol{g}$
26 $\quad\quad\quad \boldsymbol{\delta d_{gy}} \leftarrow [\boldsymbol{U}]^{-1}\,\textbf{aux}_2$
27 $\quad\quad\quad \delta\lambda_2 \leftarrow -\dfrac{(\boldsymbol{\Delta d}^{(0)T}\boldsymbol{\delta d_g})}{(\boldsymbol{\Delta d}^{(0)T}\boldsymbol{\delta d_r})}$
28 $\quad\quad\quad \boldsymbol{\delta d}_2 \leftarrow \delta\lambda_2\boldsymbol{\delta d_r} + \boldsymbol{\delta d_{gy}} - \dfrac{(\boldsymbol{\delta d_{gy}} + \delta\lambda_2\boldsymbol{\delta d_r})^T\boldsymbol{\delta d_r}}{\boldsymbol{\delta d_r}^T\boldsymbol{\delta d_r}}\boldsymbol{\delta d_r}$
29 $\quad\quad\quad \boldsymbol{\Delta d} \leftarrow \boldsymbol{\Delta d} - \boldsymbol{\delta d}_1 + \boldsymbol{\delta d}_2$
30 $\quad\quad\quad \Delta\lambda \leftarrow \Delta\lambda + \delta\lambda_2$
31 $\quad\quad\quad \boldsymbol{g} \leftarrow (\lambda + \Delta\lambda)\boldsymbol{F_r} - \boldsymbol{F_{int}}(\boldsymbol{d} + \boldsymbol{\Delta d})$
32 $\quad\quad\quad$ **if** $||\boldsymbol{g}|| < \text{aux}_1$ **or** $||\boldsymbol{\delta d}_2|| < tol_2||\boldsymbol{\Delta d}||$ **then**
33 $\quad\quad\quad\quad$ Exit the loop
34 $\quad\quad\quad$ **end**
35 $\quad\quad$ **end**
36 $\quad\quad$ **if** $k = k_{max}$ **then**
37 $\quad\quad\quad$ messagebox ('Not Converged')
38 $\quad\quad\quad$ Exit the loop
39 $\quad\quad$ **end**
40 $\quad\quad \boldsymbol{d} \leftarrow \boldsymbol{d} + \boldsymbol{\Delta d}$
41 $\quad\quad \lambda \leftarrow \lambda + \Delta\lambda$
42 $\quad\quad \boldsymbol{u} \leftarrow \boldsymbol{d} - {}^{0}\boldsymbol{d}$
43 $\quad\quad \Delta l \leftarrow {}^{0}\Delta l\left(\dfrac{Nd}{k}\right)^{0.5}$
44 $\quad\quad k_{total} \leftarrow k_{total} + k$
45 $\quad$ **end**
46 $\quad k_{av} \leftarrow \dfrac{k_{total}}{LS}$
47 $\quad t \leftarrow$ toc() (reads the timer)
48 **end**

Positional Finite Element Formulation

This section describes the 3D truss bar element using the Positional Finite Element formulation originally proposed by Coda and Greco (2004). The bar element has constant area A and transmits axial forces only. In its initial configuration, the global nodal coordinates of the truss member are defined as (X_1, Y_1, Z_1) for node 1 and (X_2, Y_2, Z_2) for node 2. Moreover, its original length (L_0) is determined by:

$$L_0 = \sqrt{(X_2 - X_1)^2 + (Y_2 - Y_1)^2 + (Z_2 - Z_1)^2}. \quad (27)$$

As for its current configuration, the global nodal coordinates of the truss member are (x_1, y_1, z_1) for node 1 and (x_2, y_2, z_2) for node 2, and its current length (L) is:

$$L = \sqrt{(x_2 - x_1)^2 + (y_2 - y_1)^2 + (z_2 - z_1)^2}. \quad (28)$$

Table 1 shows the equations of the internal force vector $\boldsymbol{F_{elem}}$ and stiffness matrix $\boldsymbol{K_{elem}}$ for the 3D truss element referring to the Engineering (ε_E), Green-Lagrange (ε_G) and Logarithmic (ε_L) strains. The matrix $\boldsymbol{K_{elem}}$ is determined by equation (29) :

$$\boldsymbol{K_{elem}} = \boldsymbol{K_M} + \boldsymbol{K_G}, \quad (29)$$

where $\boldsymbol{K_M}$ is material stiffness matrix and $\boldsymbol{K_G}$ is the geometric stiffness matrix.

In the equations shown in Table 1, E is the longitudinal modulus of elasticity and the vector $\boldsymbol{m}$ is given by equation (30):

$$\boldsymbol{m} = \begin{bmatrix} dx & dy & dz & -dx & -dy & -dz \end{bmatrix}^T, \quad (30)$$

where $dx = x_1 - x_2$, $dy = y_1 - y_2$ and $dz = z_1 - z_2$.

The differential $\dfrac{\partial \boldsymbol{m}}{\partial \boldsymbol{x}}$ is:

$$\frac{\partial \boldsymbol{m}}{\partial \mathbf{x}} = \begin{bmatrix} \boldsymbol{I_3} & -\boldsymbol{I_3} \\ -\boldsymbol{I_3} & \boldsymbol{I_3} \end{bmatrix}, \quad (31)$$

where $\boldsymbol{I_3}$ is the three-order identity matrix.

Results and discussion

This section presents the numerical results of truss problems found in the literature regarding the geometrically nonlinear static analysis. Our algorithm was run on an Intel Core i7 - 10510U CPU@1.80 GHz 2.30 GHz computer with 8 GB of memory and equipped with the free program Scilab, *version 6.1.1* (SCILAB, 2021). The analysis ignores the weight of the structures. Mesh generation and results visualization are not computed within the processing time. As our goal was to verify the effectiveness of the proposed algorithm, the system of units of the numerical examples were kept the same as the original reference.

In the nonlinear analysis methodology, the incremental-iterative procedure proposed with the method of Kou, Li and Wang (2006) and that of Newton-Raphson (RIKS, 1972; WEMPNER, 1971) are associated with the Linear Arc-Length path-following technique.

Star dome truss

The star dome truss, shown in Figure 2, contains 24 finite elements and 13 nodes. Constants $E = 1.0$ kN/cm^2 $(= 1.0 \times 10^4$ kN/m$^2)$ and $A = 1.0$ cm^2 $(= 1.0 \times 10^{-4}$ m$^2)$ were adopted for each bar.

Figure 2 – Structural model of the star dome truss.

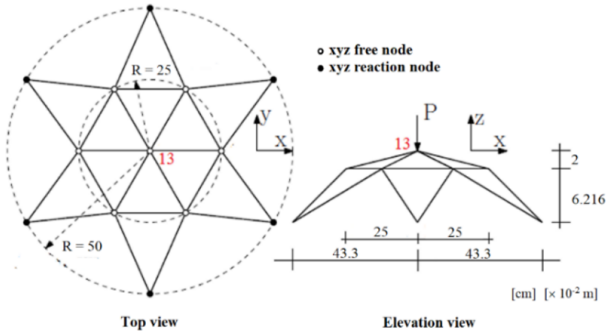

Source: The authors.

Figure 3 plots the center node equilibrium path of the structural system obtained with the proposed method (Normal Flow), evincing that the obtained results are in line with the solution provided by Yaw (2011).

Figure 3 – Star dome truss: equilibrium path.

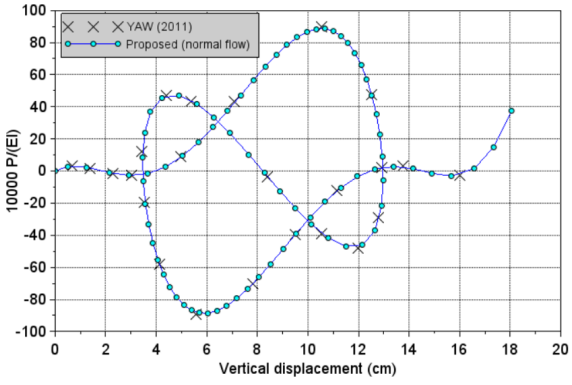

Source: The authors.

Table 1 – Formulas of the internal force vector and stiffness matrix for strain measurements.

Strain	$\boldsymbol{\varepsilon}$	$\boldsymbol{F}_{elem}$	$\boldsymbol{K}_{elem} = \boldsymbol{K}_M + \boldsymbol{K}_G$	
			$\boldsymbol{K}_M$	$\boldsymbol{K}_G$
Engineering	$\frac{L-L_0}{L_0}$	$\frac{EA\varepsilon_E}{L}\boldsymbol{m}$	$\frac{EA}{L^3}\boldsymbol{m}\boldsymbol{m}^T$	$\frac{EA\varepsilon_E}{L}\frac{\partial \boldsymbol{m}}{\partial x}$
Green-Lagrange	$\frac{L^2-{L_0}^2}{2{L_0}^2}$	$\frac{EA\varepsilon_G}{L_0}\boldsymbol{m}$	$\frac{EA}{{L_0}^3}\boldsymbol{m}\boldsymbol{m}^T$	$\frac{EA\varepsilon_G}{L_0}\frac{\partial \boldsymbol{m}}{\partial x}$
Logarithmic	$ln\left(\frac{L}{L_0}\right)$	$\frac{EAL_0\varepsilon_L}{L^2}\boldsymbol{m}$	$\frac{EAL_0}{L^4}(1-2\varepsilon_L)\boldsymbol{m}\boldsymbol{m}^T$	$\frac{EAL_0\varepsilon_L}{L^2}\frac{\partial \boldsymbol{m}}{\partial x}$

Source: The authors.

Figure 4 shows the deformed position of the truss for $LS = 80$, indicating the bars that are in traction (blue color) and in compression (red color).

Figure 4 – Star dome truss: deformed position.

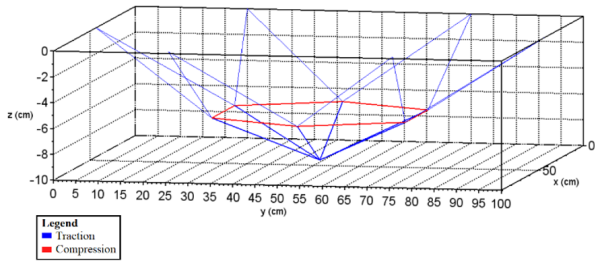

Source: The authors.

The parameters considered for the solution methods were: ${}^0\Delta l = 0.5$; $Nd = 7$; $tol_1 = tol_2 = 1.0 \times 10^{-10}$; k_{max} =150; and $\Delta P = 1.0$ N, and Table 2 shows the numerical results (LS, k_{total}, k_{av} and t). This analysis was focused on the engineering strain.

Table 2 – Numerical results for star dome truss, number of system unknowns = 40.

Algorithm	LS	k_{total}	k_{av}	$t(s)$
Proposed (conventional)	66	135	2.04	3.36
Proposed (normal flow)	80	238	2.97	5.27
NR (conventional)	79	236	2.98	4.46
NR (normal flow)	86	297	3.45	5.53
MNR (conventional)		Not converged		
MNR (normal flow)		Not converged		

Source: The authors.

Dome-shaped truss

Figure 5 shows the geometry, loading, and material properties of the dimensionless dome-shaped truss, which contains 25 nodes and 60 bar elements. For this analysis, the Green-Lagrange strain was considered.

Figure 5 – Geometry, loading and material properties of the dome-shaped truss.

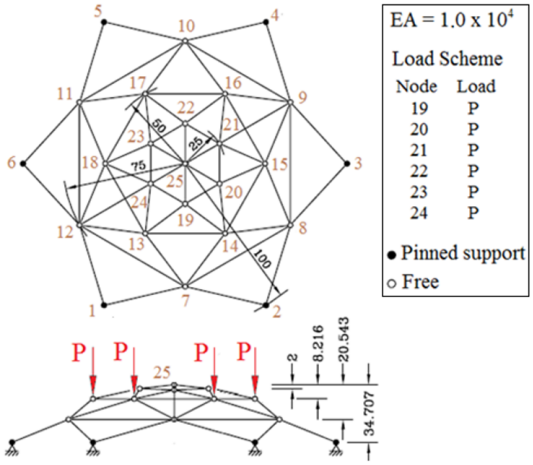

Source: The authors.

Figure 6 shows the equilibrium path (vertical displacement at node 25 versus load P), indicating a strong correlation between the curve obtained with the algorithm and the solution provided by Matias (2002).

Figure 6 – Dome-shaped truss: equilibrium path.

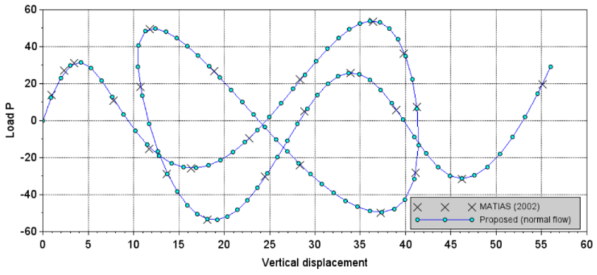

Source: The authors.

Figure 7 presents the truss deformed position for $LS = 102$, obtained with the proposed algorithm considering the Normal Flow technique.

The parameters considered for the solution methods were: ${}^0\Delta l = 4.0$; $Nd = 5$; $tol_1 = tol_2 = 1.0 \times 10^{-10}$; k_{max} =150; and $\Delta P = 0.1$, and Table 3 shows the numerical results (LS, k_{total}, k_{av} and t).

Figure 7 – Dome-shaped truss: deformed position.

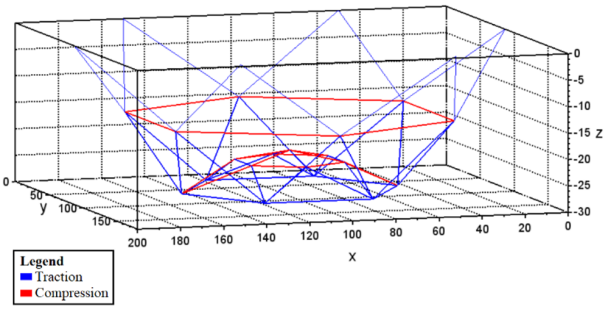

Source: The authors.

Table 3 – Numerical results for dome-shaped truss, number of system unknowns = 76.

Algorithm	LS	k_{total}	k_{av}	$t(s)$
Proposed (conventional)	100	303	3.03	22.77
Proposed (normal flow)	102	309	3.02	24.12
NR (conventional)	112	431	3.84	25.71
NR (normal flow)	114	443	3.88	27.95
MNR (conventional)		Not converged		
MNR (normal flow)		Not converged		

Source: The authors.

Circular arch truss

The circular arch truss shown in Figure 8 contains 101 elements and 42 nodes. The bars have axial stiffness $EA = 1.0 \times 10^7$ lb ($\cong 4.4482 \times 10^7$ N) and the load P is applied at the apex of the structure. This problem was proposed by Crisfield (1991) and studied by Hrinda (2010), among other authors.

Figure 8 – Structural model of the circular arch truss.

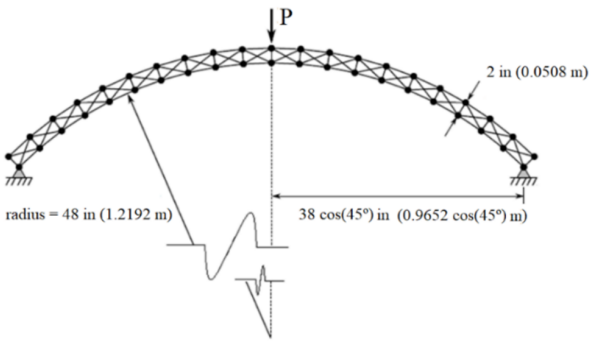

Source: The authors.

The out-of-plane motion has been constrained with pin supports added to each end of the truss. As shown in Figure 9, the equilibrium path of the structural system, vertical displacement versus load P at the apex, is complex and it has several limit points of force and displacement.

Figure 9 – Equilibrium path of the circular arch truss.

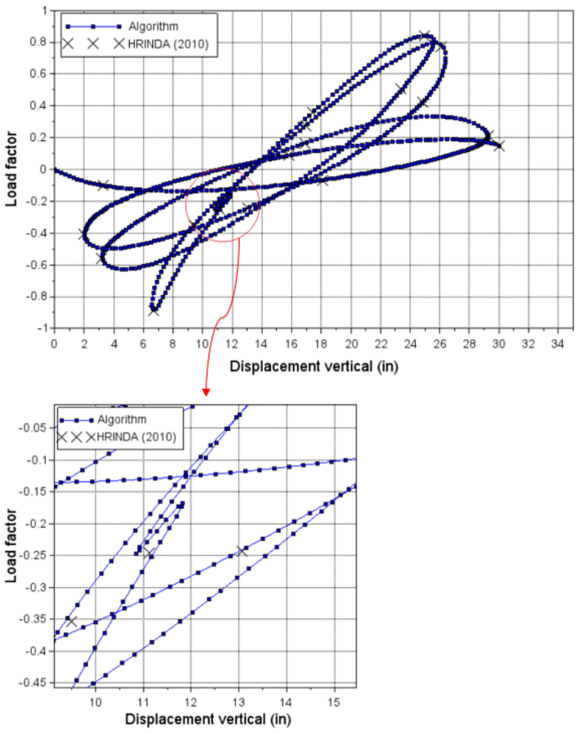

Source: The authors.

Our algorithm obtained satisfactory results for the equilibrium points of the system, corroborating those reported by Hrinda (2010). The analysis was focused on the engineering strain, and the parameters considered for the solution methods were ${}^0\Delta l = 0.5$; $Nd = 6$; $tol_1 = tol_2 = 1.0 \times 10^{-6}$; $k_{max} = 150$; and $\Delta P = 1.0 \times 10^6$ lb ($\cong 4.4482 \times 10^6$ N). Table 4 shows the numerical results (LS, k_{total}, k_{av} and t), and Figure 10 displays the arch deformed shapes for the load steps $LS = 0$, 100, 200, 300, 400 and 697, obtained with the proposed algorithm considering the Normal Flow technique.

Table 4 – Numerical results for circular arch truss, number of system unknowns = 85.

Algorithm	LS	k_{total}	k_{av}	$t(s)$
Proposed (conventional)		Not converged		
Proposed (normal flow)	697	1126	1.61	98.34
NR (conventional)		Not converged		
NR (normal flow)	750	1382	1.84	99.22
MNR (conventional)		Not converged		
MNR (normal flow)		Not converged		

Source: The authors.

Figure 10 – Deformed shapes of the circular arch truss.

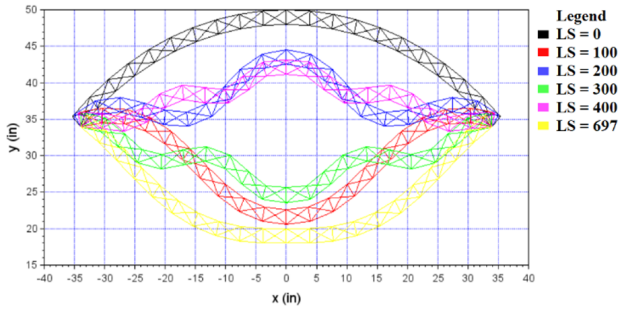

Source: The authors.

Discussion of results

The structures analyzed in this article are characterized by a nonlinear behavior, in which equilibrium paths exhibit force limit points, or maximum and minimum points, and displacement limit points, where the tangent at these points is vertical. Considering that structures may become unstable once their limit points are reached, identifying these points is of great importance for engineering designs.

When compared with standard and modified Newton-Raphson methods, the incremental-iterative procedure proposed in our study – adapted from the method developed by Kou, Li and Wang (2006) – required a smaller number of load steps and cumulative iterations for convergence to the approximate solution, independently of the technique used for the $\boldsymbol{\delta d}_i^{(k+1)}$ calculation.

Two systems of linear equations generated from the Finite Element Method, calculation of $\delta \boldsymbol{d}_{\boldsymbol{r}}^{(k+1)}$ and $\delta \boldsymbol{d}_{\boldsymbol{g}}^{(k+1)}$, are solved in the standard Newton-Raphson, whereas three systems are solved in our procedure, calculation of $\delta \boldsymbol{d}_{\boldsymbol{r}}^{(k+1)}, \delta \boldsymbol{d}_{\boldsymbol{g}}^{(k+1)}$ and $\delta \boldsymbol{d}_{\boldsymbol{gy}}^{(k+1)}$. Moreover, our procedure also includes an additional update of the internal force vector $\boldsymbol{F}_{\boldsymbol{int}}$.

The solution convergence with the modified Newton-Raphson was impaired in the numerical examples due to numerical instabilities. As in this method the stiffness matrix K is computed only at the beginning of each load step, $k = -1$, remaining invariable along the iterative cycle, nonlinear analyses can entail convergence problems. The incremental and iterative scheme of the modified Newton-Raphson method, considering the Normal Flow technique for the calculation of $\delta \boldsymbol{d}^{(k+1)}$, is given by:

$$\delta \boldsymbol{d}^{(k+1)} = \delta \boldsymbol{d}_{\boldsymbol{g}}^{(k+1)} + \delta\lambda^{(k+1)} \delta \boldsymbol{d}_{\boldsymbol{r}}^{(0)} - \frac{\left(\delta \boldsymbol{d}_{\boldsymbol{g}}^{(k+1)} + \delta\lambda^{(k+1)} \delta \boldsymbol{d}_{\boldsymbol{r}}^{(0)}\right)^T \delta \boldsymbol{d}_{\boldsymbol{r}}^{(0)}}{\delta \boldsymbol{d}_{\boldsymbol{r}}^{(0)^T} \delta \boldsymbol{d}_{\boldsymbol{r}}^{(0)}} \delta \boldsymbol{d}_{\boldsymbol{r}}^{(0)}, \qquad (32)$$

where

$$\delta \boldsymbol{d}_{\boldsymbol{g}}^{(k+1)} = -\left[\boldsymbol{K}\left(\boldsymbol{d}^{(0)}\right)\right]^{-1} \boldsymbol{g}\left(\boldsymbol{d}^{(k)}, \lambda^{(k)}\right), \qquad (33)$$

$$\delta \boldsymbol{d}_{\boldsymbol{r}}^{(0)} = \left[\boldsymbol{K}\left(\boldsymbol{d}^{(0)}\right)\right]^{-1} \boldsymbol{F}_{\boldsymbol{r}}. \qquad (34)$$

Convergence using this method can be achieved by decreasing the value of the initial arc length increment ($^0\Delta l$) and/or the number of iterations required (Nd).

With regard to the analysis of the circular arch truss, the consideration of the Normal Flow technique guaranteed the convergence for the problem solution, with obtaining a highly nonlinear equilibrium path with several limit points. Even doing additional tests with reducing of the values of $^0\Delta l$ and Nd for both solution methods, proposed and NR, the conventional technique was not able to obtain the complete solution. Non-convergence occurs at the fourth displacement limit point, Figure 11, for the proposed method and for the NR method, at the third displacement limit point, Figure 12.

Figure 11 – Point of non-convergence on the path for the proposed method.

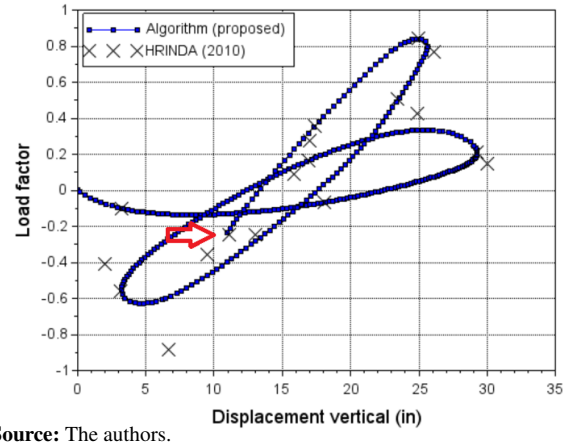

Source: The authors.

Figure 12 – Point of non-convergence on the path for the NR method.

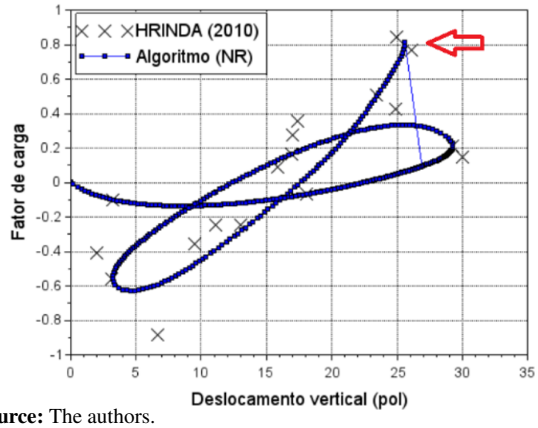

Source: The authors.

Despite ensuring convergence in all the examples studied here, the Normal Flow technique in the analysis of space trusses (star dome truss and dome-shaped truss) cannot reduce the total number of iterations (k_{total}) compared to the conventional method, as shown in Tables 2 and 3.

The sign of the initial load increment $\Delta\lambda^{(0)}$ can be either positive or negative. Determining the correct signal is key for establishing sequence solutions ($\boldsymbol{d}$, λ) that allow a continuous advance in the load-displacement response. To verify the sign change of the load increment when crossing limit points (lines 9 to 11 of the algorithm in Algorithm), we adopted an easy-to-implement and suitable technique proposed by Krenk and Hededal (1995).

The stiffness matrix $\boldsymbol{K}$ of the structural system is characterized by a high sparsity degree. Figure 13 shows the distribution of the non-null elements of the matrix $\boldsymbol{K}$ for the 42-Member Space Truss, using Scilab's *sparse*(K) and *PlotSparse*(K) functions, where nnz is the number of non-zero entries in the matrix. The sparsity degree of this matrix is 83.72%. The numerical efficiency of the proposed procedure may be enhanced by using algorithms that store non-null coefficients present in the matrix and perform operations between matrices and vectors with these coefficients, thus avoiding redundant calculations with null elements. The "sparse" function is used to build a sparse matrix in the Scilab program, and only non-null entries are stored.

Figure 13 – Distribution of non-zero elements of the stiffness matrix.

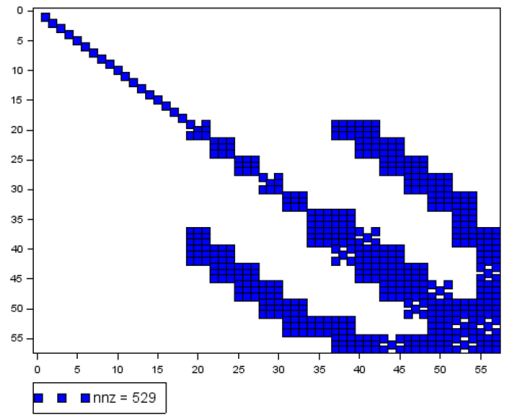

Source: The authors.

Figure 14(a)-(b) shows the percentage reduction of the total number of iterations of the new algorithm presented in Algorithm in relation to the standard Newton–Raphson method, using conventional and Normal Flow techniques, respectively.

Figure 14 – Reduction percentage of iteration: (a) Conventional technique and (b) Normal Flow technique.

(a)

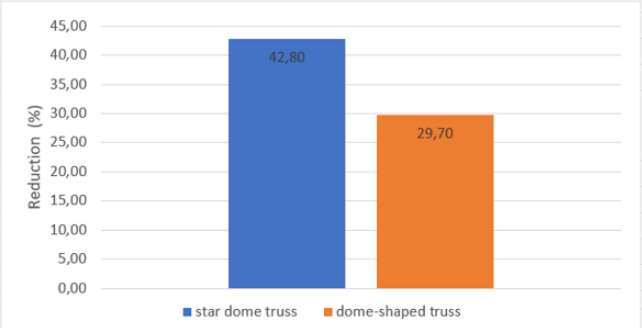

(b)

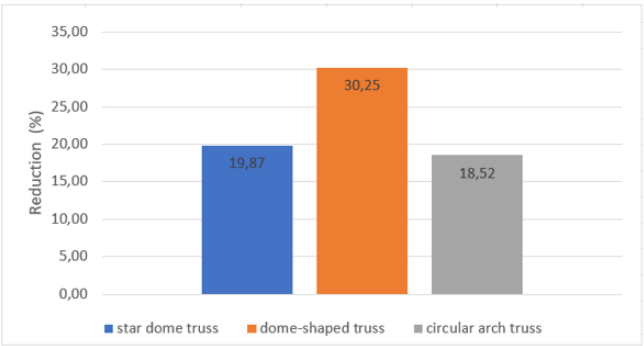

Source: The authors.

Conclusion

This study proposed a new algorithm based on the Positional Finite Element method to analyze the geometrical nonlinearity of plane and spatial trusses. The system of nonlinear equations was solved by adapting the two-step method proposed by Kou, Li and Wang (2006) and the Linear Arc-Length path-following technique into an incremental-iterative procedure. After presenting the iterative formulation, we developed a computational algorithm using the free program Scilab. The numerical examples reached satisfactory results in reducing computing time, reducing the number of the iterations, and obtaining sufficiently accurate results. As shown in trusses load-displacement curves, our algorithm was able to identify and cross the force and displacement limit points, thus being of practical interest for Structural Engineering. Moreover, it can compete and excel the Newton–Raphson method.

Acknowledgments

The authors thank the Federal Technological University of Paraná and the Graduate Program in Civil Engineering - PCV of the State University of Maringá for their support in the development of this research.

References

ALLGOWER, E. L.; GEORG, K. Homotopy methods for approximating several solutions to nonlinear systems of equations. *In*: FORSTER, W. (ed.). *Numerical solution of highly nonlinear problems*. Amsterdam: North-Holland, 1980. p. 253-270.

CODA, H. B.; GRECO, M. A simple FEM formulation for large deflection 2D frame analysis based on position description. *Computer methods in applied mechanics and engineering*, Amsterdam, v. 193, n. 33-35, p. 3541-3557, 2004.

CRISFIELD, M. A. *Non-linear finite element analysis of solids and structures*. Chichester: John Wiley & Sons Ltda, 1991. v. 1.

DEHGHANI, H.; MANSOURI, I.; FARZAMPOUR, A.; HU, J. W. Improved homotopy perturbation method for geometrically nonlinear analysis of space trusses. *Applied Sciences*, [Tubingen], v. 10, n. 8, p. 2987, 2020.

FELIPE, T. R.; LEONEL, E. D.; HAACH, V. G.; BECK, A. T. A comprehensive ductile damage model for 3D truss structures. *International Journal of Non-Linear Mechanics*, Amsterdam, v. 112, p. 13-24, 2019.

GRECO, M.; FERREIRA, I. P. Logarithmic strain measure applied to the nonlinear positional formulation for space truss analysis. *Finite elements in analysis and design*, Amsterdam, v. 45, n. 10, p. 632-639, 2009.

GRECO, M.; MENIN, R. C. G.; FERREIRA, I. P.; BARROS, F. B. Comparison between two geometrical nonlinear methods for truss analyses. *Structural engineering and mechanics*: An international journal, New York, v. 41, n. 6, p. 735-750, 2012.

HRINDA, G. Snap-through instability patterns in truss structures. *In*: AIAA/ASME/ASCE/AHS/ASC STRUCTURES, STRUCTURAL DYNAMICS, AND MATERIALS CONFERENCE 51., 2010, Orlando. *Proceesdings* [. . .]. Reston: AIAA, 2010. p. 2611.

KOOHESTANI, K. A hybrid method for efficient solution of geometrically nonlinear structures. *International Journal of Solids and Structures*, New York, v. 50, n. 1, p. 21-29, 2013.

KOU, J.; LI, Y.; WANG, X. A modification of Newton method with third-order convergence. *Applied Mathematics and Computation*, New York, v. 181, n. 2, p. 1106-1111, 2006.

KRENK, S.; HEDEDAL, O. A dual orthogonality procedure for non-linear finite element equations. *Computer Methods in Applied Mechanics and Engineering*, Amsterdam, v. 123, n. 1-4, p. 95-107, 1995.

LEON, S. E.; PAULINO, G. H.; PEREIRA, A., MENEZES, I. F.; LAGES, E. N. A unified library of nonlinear solution schemes. *Applied Mechanics Reviews*, New York, v. 64, n. 4, 2011.

MAHDAVI, S. H.; RAZAK, H. A.; SHOJAEE, S.; MAHDAVI, M. S. A comparative study on application of Chebyshev and spline methods for geometrically non-linear analysis of truss structures. *International Journal of Mechanical Sciences*, New York, v. 101, p. 241-251, 2015.

MATIAS, W. T. El control variable de los desplazamientos en el análisis no lineal elástico de estructuras de barras. *Revista internacional de métodos numéricos*, Barcelona, v. 18, n. 4, p. 549-572, 2002.

MAXIMIANO, D. P.; SILVA, A. R. D.; SILVEIRA, R. A. M. Iterative strategies associated with the normal flow technique on the nonlinear analysis of structural arches. *Rem*: Revista Escola de Minas, Ouro Preto, v. 67, n. 2, p. 143-150, 2014.

MOHIT, M.; SHARIFI, Y.; TAVAKOLI, A. Geometrically nonlinear analysis of space trusses using new iterative techniques. *Asian Journal of Civil Engineering*, [London], v. 21, n. 5, p. 785-795, 2020.

MUÑOZ, L. F. P.; ROEHL, D. A continuation method with combined restrictions for nonlinear structure analysis. *Finite Elements in Analysis and Design*, Amsterdam, v. 130, p. 53-64, 2017.

NOOR, M. A.; AHMAD, F.; JAVEED, S. Two-step iterative methods for nonlinear equations. *Applied mathematics and computation*, New York, v. 181, n. 2, p. 1068-1075, 2006.

RABELO, J. M.; BECHO, J. S.; GRECO, M.; CIMINI JR., C. A. Modeling the creep behavior of GRFP truss structures with Positional Finite Element Method. *Latin American Journal of Solids and Structures*, v. 15, n. 2, p. 1-18, 2018.

RAGON, S. A.; GÜRDAL, Z.; WATSON, L. T. A comparison of three algorithms for tracing nonlinear equilibrium paths of structural systems. *International journal of solids and structures*, New York, v. 39, n. 3, p. 689-698, 2002.

REZAIEE-PAJAND, M.; NASERIAN, R. Using residual areas for geometrically nonlinear structural analysis. *Ocean Engineering*, Elmsford, v. 105, p. 327-335, 2015.

RIKS, E. The application of newton's method to the problem of elastic stability. *Journal of Applied Mechanics*, New York, v. 39, p. 1060–1065, 1972.

SAFFARI, H.; MANSOURI, I. Non-linear analysis of structures using two-point method. *International Journal of Non-Linear Mechanics*, Amsterdam, v. 46, n. 6, p. 834-840, 2011.

SAFFARI, H.; MIRZAI, N. M.; MANSOURI, I.; BAGHERIPOUR, M. H. Efficient numerical method in second-order inelastic analysis of space trusses. *Journal of computing in civil engineering*, New York, v. 27, n. 2, p. 129-138, 2013.

SCILAB. *Version 6.1.1*. France: ESI Group, 2021.

SOUZA, L. A. F.; CASTELANI, E. V.; SHIRABAYASHI, W. V. I.; ALIANO FILHO, A.; MACHADO, R. D. Trusses nonlinear problems solution with numerical methods of cubic convergence order. *TEMA*, São Carlos, v. 19, p. 161-179, 2018.

SOUZA, L. A. F.; CASTELANI, E. V.; SHIRABAYASHI, W. V. I. Adaptation of the Newton-Raphson and Potra-Pták methods for the solution of nonlinear systems. *Semina*: Ciênc. Ex. Tech., Londrina, v. 42, n. 1, p. 63-74, Jan./Jun. 2021.

SOUZA, L. A. F.; SANTOS, D. F. D.; KAWAMOTO, R. Y. M.; VANALLI, L. New fourth-order convergent algorithm for analysis of trusses with material and geometric nonlinearities. *The Journal of Strain Analysis for Engineering Design*, London, v. 57, n. 2, p. 104-115, 2021.

THAI, H. T.; KIM, S. E. Large deflection inelastic analysis of space trusses using generalized displacement control method. *Journal of Constructional Steel Research*, London, v. 65, n. 10/11, p. 1987-1994, 2009.

TURCO, E.; BARCHIESI, E.; GIORGIO, I.; DELL'ISOLA, F. A Lagrangian Hencky-type nonlinear model suitable for metamaterials design of shearable and extensible slender deformable bodies alternative to Timoshenko theory. *International Journal of Non-Linear Mechanics*, Amsterdam, v. 123, p. 103481, 2020.

YAW L. L. *3D Co-rotational Truss Formulation*. Walla Walla: Walla Walla University, 2011.

WEMPNER, G. A. Discrete approximations related to nonlinear theories of solids. *International Journal of Solids and Structures*, New York, v. 7, n. 11, p. 1581-1599, 1971.

Received: May 2, 2022
Accepted: June 17, 2022
Published: June 26, 2022